

DEVELOPMENT OF A SOURCE OF FEMTOSECOND X-RAY PULSES BASED ON THE ELECTRON STORAGE RING*

A. Zholents[†], J. Byrd, S. Chattopadhyay, H. Chong, T.E. Glover, P. Heimann, R. Schoenlein, C. Shank, M. Zolotorev, LBNL, Berkeley, CA 94720

1 INTRODUCTION

The dynamic properties of materials are governed by atomic motion which occur on the fundamental time scale of a vibrational period ~ 100 fs. This is the time scale of interest for ultrafast chemical reactions, non-equilibrium phase transitions, vibrational energy transfer, surface desorption and reconstruction, and coherent phonon dynamics. To date, our understanding of these processes has been limited by lack of appropriate tools for probing atomic structure on an ultrafast time scale. The time resolution of high-brightness 3-rd generation synchrotron light sources is more than two orders of magnitude too slow for these studies. However, the desired x-ray pulses may be achieved by selecting radiation which originates from a thin ~ 100 fs temporal slice of an electron bunch.

2 LASER / E-BEAM INTERACTION

A ~ 100 fs temporal slice of an electron bunch can be created through the interaction of a femtosecond laser pulse co-propagating with an electron bunch in a wiggler magnet [1]. The high electric field present in the femtosecond laser pulse produces an energy modulation in the electrons as they traverse the wiggler (some electrons are accelerated and some are decelerated depending on the optical phase ϕ). The optimal interaction occurs when the laser wavelength λ_L satisfies the resonance condition $\lambda_L \simeq \lambda_W(1 + a_W^2/2)/2\gamma^2$ where γ is the Lorentz factor, a_W is the deflection parameter, and λ_W is the wiggler period. In addition, the far field laser radiation must overlap with the far field spontaneous radiation from the electron passing through the wiggler, and the laser spectral bandwidth (number of optical cycles per pulse, M_L) must match the spectrum of the fundamental wiggler radiation (determined by the number of wiggler periods M_W). Under these conditions, the energy absorbed by the electron from the laser field (or transferred to the laser field) is calculated by considering the energy of the superposition of the fields of laser radiation and the spontaneous electron wiggler radiation in the far field region [1]:

$$(\Delta E)^2 = 4\pi\alpha\hbar\omega_L \frac{a_W^2/2}{1 + a_W^2/2} \frac{M_W}{M_L} A_L \cos^2 \phi, \quad (1)$$

where \hbar is the Planck's constant, α is the fine structure constant, A_L is the laser pulse energy, $\omega_L = 2\pi c/\lambda_L$, and c is the speed of light. We estimate that a 35 fs laser

pulse with a photon energy $\hbar\omega_L = 1.55$ eV, and pulse energy $A_L = 100\mu\text{J}$ will produce an energy modulation $\Delta E \simeq 10$ MeV, using a wiggler with $M_W = 19$, $\lambda_W = 16$ cm, and $a_W \simeq 13$ at electron beam energy of 1.5 GeV.

Only electrons which temporally overlap with the laser pulse experience this modulation. The laser-induced energy modulation is several times larger than the rms beam energy spread in the typical 1.5 GeV electron storage ring. The accelerated and decelerated electrons are then spatially separated from the rest of the electron in the bend magnets of the storage ring by a transverse distance that is several times larger than the rms transverse size of the electron beam. Finally, by imaging the displaced beam slice to the experimental area, and by placing an aperture radially offset from the focus of the beam core, we will be able to separate out the radiation from the offset electrons. Figure 1 schematically shows all three phases of preparing the femtosecond x-ray pulses.

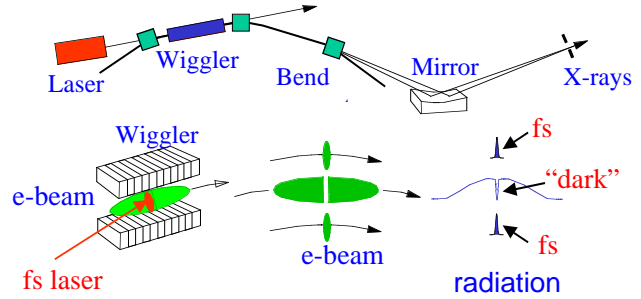


Figure 1: A schematic of generation of the femtosecond pulses of synchrotron radiation.

Since the spatially offset electrons result from interaction with the laser pulse, the duration of the synchrotron radiation produced by these electrons will be approximately the same as the duration of the laser pulse, and will be absolutely synchronized. Furthermore, the extraction of an ultrashort slice of electrons leaves behind an ultrashort hole or dark pulse in the core of the electron bunch. This time structure will be reflected in the generated x-rays by beam core electrons, and can also be used for time-resolved spectroscopy.

The average flux of the femtosecond radiation is defined by three factors: $\eta_1 = \tau_L/\tau_b$, $\eta_2 = f_L/f_b$, and $\eta_3 \simeq 0.2$, where τ_L and τ_b are the laser pulse and electron bunch durations, f_L and f_b are the laser and electron bunch repetition rates, and η_3 accounts for the fraction of electrons that are in the proper phase of the laser pulse to get the maximum energy exchange suitable for creating the large transverse separation. Taking $\tau_L = 35$ fs, $f_L = 10$ kHz and using

* Work supported by DoE under contract No DE-AC03-76SF00098.

[†] Email: AAZholents@lbl.gov

typical ALS electron beam parameters $\tau_b=30$ ps, $f_b=500$ MHz, we estimate a femtosecond x-ray flux of 3×10^5 photons/sec/0.1 % BW at 2 keV (5×10^4 photons/sec/0.1 % BW at 10 keV) from a bend-magnet beamline at the ALS with a $3 \text{ mrad} \times 0.4 \text{ mrad}$ collection optic.

Synchrotron radiation damping provides for recovery of the electron beam between interactions. Since the laser interacts sequentially with each bunch, the interaction time is given by n/f_L , where n is number of bunches in the storage ring. Furthermore, the bunch slice is only a small fraction of the total bunch. Thus, the storage ring damping time is more than sufficient to allow recovery of the electron beam between laser interactions (even for laser repetition rates as high as 100 kHz).

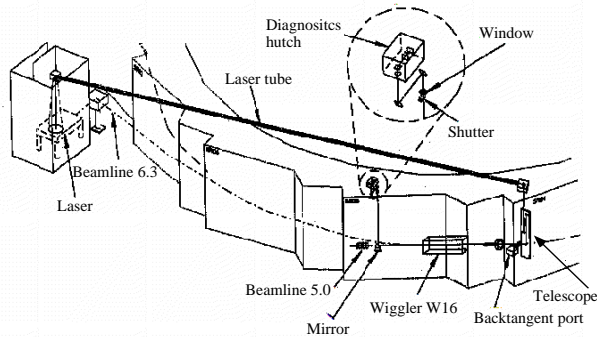


Figure 2: The layout of the experiment.

A proof of principle experiment for the technique described above has been conducted at the ALS storage ring at LBNL. A schematic of the experimental set up is shown in Figure 3. A femtosecond Ti:Sapphire laser synchronized to the storage ring is located near beamline 6.3.2, and the laser beam is projected across the storage ring roof blocks to sector 5, where it enters the main vacuum chamber through a back-tangent optical port. Amplified femtosecond laser pulses co-propagate with the electron beam through wiggler W16 in sector 5. A mirror following the wiggler reflects the laser light and the visible wiggler emission out of the vacuum chamber for diagnostic purposes. Images of the near field and far field wiggler radiation are observed on a CCD camera, and the near and far field modes of the laser propagating through the wiggler are matched using a remotely adjustable telescope at the back tangent port. The spectrum of the laser is also matched to the fundamental wiggler emission spectrum. The efficiency of the laser/e-beam interaction is tested by measuring the gain in the intensity experienced by the laser beam passing with the electron beam through the wiggler [2]. This gain is a direct indication of the magnitude of the energy exchange between the laser and the electrons. Femtosecond duration synchrotron pulses are directly measured by cross-correlating the visible light from bend-magnet beamline 6.3.2 with the synchronized laser pulses. Figure 3a shows a laser pulse and a synchrotron radiation pulse cross-

correlation measurement on a 100 ps time scale. The measured synchrotron pulse duration, $\sigma=16$ ps, corresponds to the overall electron bunch duration. Measurement with ~ 100 times higher time resolution (Figure 3b) shows the femtosecond "dark" pulse ($\sigma=112$ fs) which appears as a narrow $\sim 25\%$ deep hole in the main pulse, and originates from the central core of the sliced electron bunch. Both, the width and the height of the hole appear to be close to the expected values. The pulse duration is mainly defined by a spread of the pathlengths of the electron trajectories between the wiggler and the 6.3.2 bend-magnet. Figure 3c shows a measurement of the femtosecond pulse ($\sigma=161$ fs) originating from the spatial wings of the sliced electron bunch. Note that the femtosecond time structure is invariant over the entire spectral range of bend-magnet emission from the near infrared to the x-ray regime. An important point is that in the far infrared region ($\lambda = 100 - 300 \mu\text{m}$) the narrow hole in the electron bunch radiates coherently such that the intensity of the radiation is proportional to the square of the number of missing electrons in the hole. We estimate that this radiation carries ~ 1 nJ per pulse.

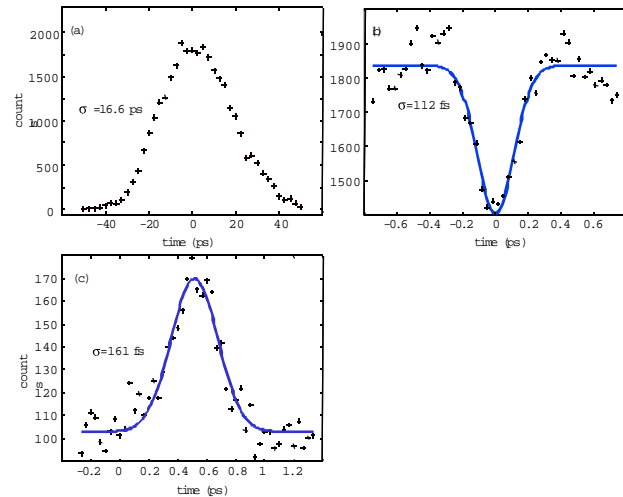


Figure 3: The measured synchrotron radiation pulses duration. See text for explanation.

3 RF ORBIT DEFLECTION

Another way to create femtosecond slices of electrons is to use the RF orbit deflection [3]. This technique implies that the femtosecond slices of the electron bunch are made by creating a correlation between the longitudinal coordinates of the electrons within the electron bunch and their vertical angles. This correlation can be initiated by the first dipole mode E_{110} of an RF cavity accelerating structure.

While passing the accelerating structure, electrons are deflected by the RF magnetic field an amount equal to:

$$y'(z) = \theta_0 \sin(kz), \quad \theta_0 = \frac{eU}{E_b}, \quad (2)$$

where z is the electron longitudinal coordinate relative to

the bunch center, E_b is the beam energy, e is the electron charge and eU is the energy gain in the accelerating structure calculated at the coordinates with the maximum electric field. It is assumed that the RF phase is chosen in a such way that $\psi = 0$ when the bunch center is at the center of the cavity.

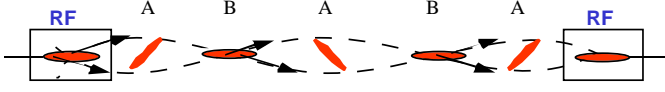


Figure 4: A schematic of the beam coupling produced by the RF cavities operated at E_{110} mode.

This deflection couples the longitudinal and transverse motion of the electrons. In order to confine this coupling in a section of a storage ring, a second accelerating structure is placed an integer number of betatron wavelengths downstream of the first accelerating structure.

Figure 4 schematically shows two accelerating structures, trajectories of the head and tail parts of the electron bunch and side views of the bunch profile in several locations as it propagates from left to right. There are two types of locations along the orbit, which are convenient source points of synchrotron radiation for our purpose. At the A locations, the coordinate displacements of the electrons have reached their maxima:

$$\delta y(z) = \theta_0 \sqrt{\beta_{rf}} \beta \sin(kz), \quad (3)$$

where β_{rf} is the vertical beta function at the RF cavity and β is the vertical beta function in the A locations. Instead, at the B locations, the variation in angle of the electron trajectories has its maximum value:

$$\delta y'(z) = \theta_0 \sqrt{\frac{\beta_{rf}}{\beta}} \sin(kz), \quad (4)$$

where β is taken now in the B locations.

For zero beam emittance we can say that the radiation of each femtosecond slice is separated from the radiation of the neighboring slices if the difference in angle or coordinate between the neighboring slices is larger than the opening angle of the radiation, $\sigma_{r'}$, in the case of the angular separation or the diffraction-limited size of the radiation, $\sigma_r = \lambda/4\pi\sigma_{r'}$, in the case of coordinate separation.

For a non-zero beam emittance we need to account for the broadening of the radiation field due to the coordinate and angular spread of electrons and consider $(\sigma_y^2 + \sigma_r^2)^{1/2}$ and $(\sigma_{y'}^2 + \sigma_{r'}^2)^{1/2}$ instead of σ_r and $\sigma_{r'}$, where σ_y and $\sigma_{y'}$ are the vertical electron beam size and divergence at the source position. This broadening is much less in the vertical direction because vertical beam emittance in the storage ring is much smaller than the horizontal emittance.

Defining the length of the femtosecond slice as σ_s and the bunch length as σ_z , we can write a magnitude $\delta y(\sigma_z)$ in the A locations and a magnitude $\delta y'(\sigma_z)$ in the B locations

needed for a spatial separation of the radiation of $M = \sigma_z/\sigma_s$ femtosecond slices:

$$\delta y(\sigma_z) \geq M(\sigma_y^2 + \sigma_r^2)^{1/2} \quad (5)$$

$$\delta y'(\sigma_z) \geq M(\sigma_{y'}^2 + \sigma_{r'}^2)^{1/2}.$$

One also needs to check that the vertical beam tilt is larger than the opening angle of the radiation, i.e. that $\arctan[\delta y(\sigma_z)/\sigma_s] > (\sigma_{y'}^2 + \sigma_{r'}^2)^{1/2}$. Usually this condition is easily satisfied.

Using Eqs.(3,4) in the left hand side of Eqs. (5), and assuming $k\sigma_z \leq 1$, we find the energy gain eU required for the creation of M femtosecond slices:

$$\frac{eU}{E_b} \geq \frac{M}{k\sigma_z} \sigma_{y'}^{rf} \sqrt{1 + \left(\frac{\sigma_r}{\sigma_y}\right)^2} \quad (6)$$

$$\frac{eU}{E_b} \geq \frac{M}{k\sigma_z} \sigma_{y'}^{rf} \sqrt{1 + \left(\frac{\sigma_{r'}}{\sigma_{y'}}\right)^2},$$

where $\sigma_{y'}^{rf} = \sqrt{\epsilon_y/\beta_{rf}}$ is the vertical angular beam size in the location of the RF cavity, and ϵ_y is the vertical beam emittance.

Compression of the radiation of all beam slices into a single x-ray pulse of the order of ~ 150 fs may be performed in the x-ray beamline. Asymmetrically-cut crystals may be used as optical elements for x-ray pulse compression [4]. Because of the different incident and diffractive angles, they produce a variable path length across the x-ray beam. Alternatively, one can use the angle-time or coordinate-time correlation of the radiation for simultaneous observation of different time delays on a position sensitive detector.

The disadvantage of the RF orbit deflection technique is a requirement of a ≤ 100 fs jitter in a synchronization of the laser to the electron beam in a storage ring. It is factor of four better than the best obtained results [5]. The advantage of this technique is that the femtosecond x-ray pulses are generated by every electron bunch and on every orbit turn and all electrons contribute to the radiation. Therefore, the resulting flux of the x-rays is many orders of magnitude higher than in the first technique ($\sim 10^{14}$ photons/sec/0.1 % BW at 5 keV for undulator radiation). However, the real flux that currently can be utilize in practice in a pump - probe measurement is approximately three orders of magnitude less because of the repetition frequency and pulse energy limitations of present femtosecond lasers.

Acknowledgement. The authors wish to acknowledge the technical support of the LBNL laser safety officer K. Barat and the staff of the ALS in setting-up this experiment.

4 REFERENCES

- [1] A. Zholents and M. Zolotarev, PRL v.76, (1996)912.
- [2] M. Zolotarev, et. al. in Proc. of this Conf., reprint WEP102.
- [3] A. Zholents, et. al., LBNL-42045, to be published in NIM.
- [4] T. Matsushita and H. Hashizume, Handbook of Synchrotron Radiation v.1, ed. E.E. Koch, p.261, Amsterdam (1993).
- [5] G.M.H. Knippels, et.al., abstract at 20th FEL Conf., 1998.